Volume 1 | Number 1 | Jan 2013 | Pages 1–100

MedChemComm

www.rsc.org/medchemcomm

pDOS

ROYAL SOCIETY OF CHEMISTRY

EFMC
European Federation for Medicinal Chemistry

This is an *Accepted Manuscript*, which has been through the Royal Society of Chemistry peer review process and has been accepted for publication.

Accepted Manuscripts are published online shortly after acceptance, before technical editing, formatting and proof reading. Using this free service, authors can make their results available to the community, in citable form, before we publish the edited article. We will replace this *Accepted Manuscript* with the edited and formatted *Advance Article* as soon as it is available.

You can find more information about *Accepted Manuscripts* in the **Information for Authors**.

Please note that technical editing may introduce minor changes to the text and/or graphics, which may alter content. The journal's standard **Terms & Conditions** and the **Ethical guidelines** still apply. In no event shall the Royal Society of Chemistry be held responsible for any errors or omissions in this *Accepted Manuscript* or any consequences arising from the use of any information it contains.

Structure of the Cannabinoid Receptor 1: Homology Modeling of Its Inactive State and Enrichment Study Based on CB1 Antagonist Docking

Haining Liu, Ronak Y. Patel, Robert J. Doerksen[*]

Department of Medicinal Chemistry, School of Pharmacy, University of Mississippi, University MS 38677 USA

Email: rjd@olemiss.edu

2

Abstract Cannabinoid receptor 1 (CB1) antagonists have potential to be used clinically to treat obesity, but there are currently no such drugs on the market. Since no X-ray crystal structure is available for CB1, considerable attempts have been made to prepare CB1 protein homology models, but in this work we propose a new CB1 inactive state model which is specific to CB1 antagonists, as validated by its enrichment performance. We first built multiple CB1 homology models. The enrichment performance of these models was then systematically examined using two datasets. A small dataset that contains 72 highly active CB1 antagonists was docked into these models. Only one of the models was able to dock all the compounds. After minimization and followed by redocking, two more models were able to dock all the 72 compounds. Next, a large dataset that contains 181 active CB1 antagonists and 3439 inactive CB1 antagonists/decoy compounds was used to assess the enrichment performance of the 3 models. One of the models was found to have much better enrichment performance than the other 2 models. This best CB1 model will be used in future virtual screening studies.

1. Introduction

The cannabinoid receptors are G-protein coupled receptors (GPCR). There are two known receptor subtypes, CB1 and CB2,[1] though increasing evidence now suggests that a third subtype may exist.[2, 3] The localizations of CB1and CB2 are primarily in the central nervous system[4, 5] and immune system,[6, 7] respectively. Recently, attempts to discover novel ligands that are able to bind to CB receptors (CBrs) have attracted considerable interest, due in part to the important physiological roles that CBrs play *in vivo*.[8-10] For example, it is known that CB1 antagonists can be used to treat obesity[11] and CB2 agonists can be used to treat pain.[12] Although a number of CB ligands with quite different skeletons have been reported,[7, 13-16] investigations to discover novel CB ligands are of great importance and interest. However, the lack of experimentally determined crystal structures of CBrs has significantly hampered the progress of the discovery of CB ligands using protein structure-based approaches, which, as a result, makes ligand-based approaches, such as pharmacophore modeling[17] and quantitative structure-activity relationship models,[18, 19] more popular in this field.

We are interested in the discovery of novel CB1 ligands using protein structure-based methods. So far, several CB1 model structures have been reported in the literature.[20] Most of these studies used the crystal structure of bovine rhodopsin as the template, including the works by Shim and coworkers in 2003[21] and 2008,[22] Salo and coworkers in 2004,[23] Páez and coworkers in 2005,[24] Martinelli and coworkers in 2006,[25] and Gonzalez and coworkers in 2008.[26] By contrast, the more recently reported crystal structures of the β_2-adrenergic receptor and human adenosine A_{2A} receptor were used as the template by Shim and coworkers in 2009,[27] and Chang and coworkers in 2012.[28] In some of these studies, the obtained models were relaxed by molecular dynamics methods, and well known CB1 ligands, such as WIN55212-2,[25, 28] anandamide (AEA),[23, 25] 2-arachidonoylglycerol (2-AG)[23] and CP55244,[22] were docked into the protein binding site to further assess the value of the obtained structure models. In addition, the homology models were used for virtual screening to identify new CB1 antagonists.[29] However,

4

there has still been a lack of systematic examination of the enrichment performance of CB1 models, an important measure of the potential value of the models for use in virtual screening studies. One way to test if models will be efficient for discovery of new CB1 ligands is to examine the ability of the models to enrich the selection of known active CB1 ligands from a large dataset of inactive and decoy compounds. In this work, we report a new strategy to build multiple homology models of the CB1 inactive state, and we assessed the enrichment performance of the models to retrieve active CB1 antagonists from a large dataset. The best obtained model will be suitable for future virtual screening studies.

2. Computational methods

Sequence alignment

We modeled the CB1 structure from V71–L472, as done by Páez and coworkers,[24] because the first 70 amino acid residues, which belong to the long CB1 N-terminus, are thought not to play any role in ligand binding.[30, 31] The crystal structure of bovine rhodopsin (PDB: 1F88) was used as the template. The alignments of the transmembrane (TM) regions, TM1, TM2, TM3, TM4, TM6 and TM7, were taken from Shim and coworkers' study.[21] For TM5, we used the alignment reported by Tuccinardi and coworkers.[25] Because TM5 in CB1 lacks the highly conserved proline residue, a gap was inserted at that position according to the method used in Tuccinardi and coworkers' study.[25] The N-terminus, IL1, EL1, IL2 and EL3 were aligned using CLUSTALW,[32] with the Blosum matrix, a gap open penalty of 10 and a gap extension penalty of 0.05. The alignments of the long loops, IL3 and C-terminal were taken directly from Tuccinardi and coworkers' study.[25] The EL2 in CB1, however, is significantly different from that of bovine rhodopsin.[1] In most GPCRs, a disulfide bridge is formed between EL2 and TM3,[33] which makes EL2 bend down and locate itself above the ligand binding pocket. However, this is impossible for CB1 because its TM3 does not have any cysteine residue. Hence, aligning EL2 of CB1 to that of bovine rhodopsin may not be able to yield accurate models. Therefore we modeled EL2 without any template. The overall alignment used in our study is shown in Figure 1.

Model building

Based on the above alignment, 150 CB1 homology models were generated using the Modeller software.[34] During model building, two constraints were employed. First, it has been suggested from experimental studies that C257 and C264 in the EL2 region may form a disulfide bond.[1, 35] Hence, a disulfide bond constraint between these two residues was used when building the models. In addition, it was found that D338 and R214 form a salt bridge,[36] which is important for keeping the receptor in the inactive state for antagonist binding. Hence, a harmonic distance constraint between the key heavy atoms in these residues was also employed during the model building process. After the models were obtained, Ramachandran analysis was performed using the PROCHECK program.[37]

Compound database

We built our database by collecting 223 compounds shown to be CB1 antagonists from 13 papers.[38-48] Compounds were classified as active if Ki ≤ 50 nM, or IC50 or EC50 ≤ 100 nM. Otherwise, they were classified as inactive. By using this criterion, 181 compounds were classified as active while 42 compounds were classified as inactive. For the compounds in each paper, except those in the work by Pinna and coworkers[48] in which no active CB1 ligands were reported, the six most active compounds were selected to form dataset I for a small scale enrichment study. This dataset hence has in total 72 compounds.

A second dataset was then made to use for a large scale enrichment study. A total of 3397 compounds, whose molecular weight, number of hydrogen bond donors, number of hydrogen bond acceptors and number of rotatable bonds are in the same of range as those of the above 223 compounds, were randomly selected from the Asinex Gold Collection database. These 3397 compounds, which we assumed to be inactive and thus labeled as inactive, were combined with the 223 CB1 antagonists to form dataset II. This dataset has in total 3620 compounds, of which 181 (5%) were active.

Docking

All docking calculations were performed using the Glide software.[49] The standard precision (SP) module in Glide was used. The residue W279 was set as the central point for Glide docking. In addition, a hydrogen bond constraint was set on K192 during docking, because it has been shown in several studies that this residue is crucial for CB1 ligand binding.[1, 50-53]

3. Results and discussion

Homology modeling

Figure 2 shows the superposition of the 150 CB1 models generated from Modeller. It can be seen that these models cover a large degree of the conformational freedom of the receptor. In particular, the loops show much more conformational variability than the transmembrane regions. In addition, the sidechains of the transmembrane regions have a greater conformational freedom than the backbones. These models hence cover a large portion of the conformational space of the receptor, while maintaining the overall fold of the protein, which can be beneficial features when considering their suitability for use in docking and/or virtual screening studies.

We also performed Ramachandran analysis using the PROCHECK program on the 150 obtained models. The results are listed in Table S1. For all the models, the residues in the most favored, additionally allowed, generally allowed and disallowed regions are in the range of 85.3%–91.7%, 6.7%–12.3%, 0.3%–2.7% and 0%–1.6%, respectively. In addition, the overall PROCHCECK scores are in the range of −0.17 to +0.33, which are well above the acceptable PROCHECK score of −0.5. Hence, these statistical results show that all of the obtained 150 models are geometrically reasonable.

Enrichment study

We first performed an enrichment study using dataset I, which has 72 compounds. Because the compounds in dataset I were selected from the most active ones in each published paper, and the reported highest IC50 from among them is only 64.7 nM, we set as a criterion that a

reasonable CB1 model should be able to dock all these 72 compounds. After docking, only 1 out of the 150 models met this criterion. In addition, 11 of the models could not dock any of the ligands. A possible reason is that the above homology models were not relaxed. In order to allow the protein to be relaxed, for each of the models together with its best-scoring docked compound, a minimization was performed using the OPLS2005 force field as implemented in the MacroModel program.[54] After that, all of the 72 compounds were redocked into the relaxed protein models. This time, 2 different models successfully docked all of the 72 compounds. The numbers of compounds that could be docked into each non-minimized and minimized model are provided in Table S2 and a graphical illustration is shown in Figure 3. It is interesting to note that these 2 models were different from the previous model that could, before being relaxed, dock all the 72 compounds. In other words, the model that was able to dock all the compounds before geometry minimization failed to do so after minimization. This may be due to the significant induced-fit effects for the protein, in which during the minimization the protein structure adapts its local structure to be appropriate for the particular ligand that is located in the binding pocket. This can allow the binding pocket to undergo significant changes, rendering the model unable to accommodate other ligands.

After the above filtration, three models were left, one from the non-minimized and two from the minimized homology models. We then performed an enrichment study on the three models using a large dataset II containing 3620 compounds. The enrichment curves for the models are shown in Figure 4. It can be clearly seen that the performance of two of the models was even worse than random selection. Only one model had a reasonable performance in the enrichment study, which was one of the minimized models. In the top 20% of the hits, for the best model, 91 CB1 antagonist compounds (50.3%) were retrieved. This hence indicates the importance of evaluating the enrichment capabilities of the models and the importance of the relaxation of homology models to be used in virtual screening. The three-dimensional structure of this best model is available in PDB format in the Supplementary Information.

Protein-ligand interactions

So far, neither the crystal structure of CB1 itself nor that of CB1 with a co-crystallized ligand is available. One of the best studied CB1 antagonists is rimonabant. It has been found from mutagenesis studies that the key residues involved in rimonabant binding to CB1 are K192, which forms a hydrogen bond with the carboxamide oxygen,[51] and W279-W356-F200, which form hydrophobic interactions with rimonabant.[53] To further validate our model, rimonabant was docked into the best model and the obtained protein–ligand complex was further minimized using the OPLS2005 force field as implemented in the MacroModel program.[54] The final binding mode is shown in Figure 5 (and is given in PDB format in the Supplementary Information). It can be seen that the obtained binding mode matches well with previous findings. For example, the hydrogen bonding interaction between K192 and the carboxamide oxygen of rimonabant was observed. In addition, the aromatic moiety of rimonabant forms hydrophobic interactions with W279-W356-F200. Therefore, this shows the reliability of our obtained model to study the interactions between CB1 antagonists and the protein.

Figures 6 and 7 show the binding modes of two typical ligands from dataset I. The ligand in Figure 6 has the best docking score among all the ligands in dataset I. The experimentally measured IC50 of this ligand is 1.96 nM.[46] In addition, it contains a carboxamide functional group similar to rimonabant. It can be seen from Figure 6 that the carboxamide again forms a hydrogen bond with K192. In addition, the (4-chlorophenyl)cyclopropyl moiety hydrophobically interacts with W279-W356-F200. Furthermore, there are several other hydrophobic residues in the binding pocket, such as F379, L359, M363, L193 and L276, which help the stabilization of the ligand via hydrophobic interactions.

The ligand shown in Figure 7 has an experimentally measured IC50 of 6.57 nM.[40] Different from rimonabant, it does not have a carboxamide functional group. However, a nitrogen atom from the thiadiazole moiety of the ligand still forms a hydrogen bond with K192. In addition, hydrophobic interactions between the ligand and W279-W356-F200 were again observed. Hence, all these docking studies show that our model is able to reproduce the well-known key

interactions between CB1 antagonists and the protein, which further validates the reliability of our model.

4. Conclusions

The work reported in this study provides a new strategy to develop useful homology models that can be applied for virtual screening purpose. We first built multiple CB1 homology models. These models were then systematically examined based on their docking performance. Using a small dataset that has 72 active CB1 antagonist compounds, only one model was found to be able to dock all the 72 compounds. After minimization by the OPLS2005 force field to allow the protein to relax, two more models were found to be able to dock all the 72 compounds. These three models were then assessed in enrichment studies using a large dataset containing 3620 compounds, in which 5% were known active CB1 antagonists. One of the models showed the best enrichment performance to retrieve the known actives at a significant rate. Rimonabant, one of the best studied CB1 antagonists, was then docked into this model and the obtained docking pose matches well with previous experimental mutagenesis studies. The obtained best CB1 model is expected to be useful for virtual screening to discover novel CB1 antagonists.

Supplementary Information. The best CB1 homology model is available in PDB format. Also available is the best CB1 model after rimonabant docking and minimization.

References

1. P. H. Reggio, *Curr. Med. Chem.*, 2010, **17**, 1468-1486.
2. E. Fride, A. Foox, E. Rosenberg, M. Faigenboim, V. Cohen, L. Barda, H. Blau and R. Mechoulam, *Eur. J. Pharmacol.*, 2003, **461**, 27-34.
3. F. Petitet, M. Donlan and A. Michel, *Chem. Biol. Drug Des.*, 2006, **67**, 252-253.
4. M. Glass, R. L. M. Faull and M. Dragunow, *Neuroscience*, 1997, **77**, 299-318.
5. T. M. Westlake, A. C. Howlett, T. I. Bonner, L. A. Matsuda and M. Herkenham, *Neuroscience*, 1994, **63**, 637-652.
6. S. Munro, K. L. Thomas and M. Abu-Shaar, *Nature*, 1993, **365**, 61-65.
7. G. G. Muccioli and D. M. Lambert, *Curr. Med.Chem.*, 2005, **12**, 1361-1394.
8. P. P. Basu, M. M. Aloysius, N. J. Shah and R. S. Brown Jr, *Alimentary Pharmacology and Therapeutics*, 2014.
9. L. E. Klumpers, C. Roy, G. Ferron, S. Turpault, F. Poitiers, J. L. Pinquier, J. G. C. van Hasselt, L. Zuurman, F. A. S. Erwich and J. M. A. van Gerven, *British Journal of Clinical Pharmacology*, 2013, **76**, 65-77.
10. S. Lim, J. P. Despres and K. K. Koh, *Circulation Journal*, 2011, **75**, 1019-1027.
11. U. Pagotto, V. Vicennati and R. Pasquali, *Ann. Med.*, 2005, **37**, 270-275.
12. M. Beltramo, *Mini Rev. Med. Chem.*, 2009, **9**, 11-25.
13. S. Han, F. F. Zhang, X. Xie and J. Z. Chen, *European Journal of Medicinal Chemistry*, 2014, **74**, 73-84.
14. C. A. Lunn, *Curr. Top. Med. Chem.*, 2010, **10**, 768-778.
15. H.-K. Lee, E. B. Choi and C. S. Pak, *Curr. Top. Med. Chem.*, 2009, **9**, 482-503.
16. N. Jagerovic, C. Fernandez-Fernandez and P. Goya, *Curr. Top. Med. Chem.*, 2008, **8**, 205-230.
17. H. Wang, R. A. Duffy, G. C. Boykow, S. Chackalamannil and V. S. Madison, *J. Med. Chem.*, 2008, **51**, 2439-2446.
18. N. S. Kang, G. N. Lee and S.-E. Yoo, *Bioorg. Med. Chem. Lett.*, 2009, **19**, 2990-2996.
19. J.-Z. Chen, X.-W. Han, Q. Liu, A. Makriyannis, J. Wang and X.-Q. Xie, *J. Med. Chem.*, 2005, **49**, 625-636.
20. C. E. A. Chang, R. Ai, M. Gutierrez and M. J. Marsella, in *Methods in Molecular Biology*, 2012, pp. 595-613.
21. J.-Y. Shim, W. J. Welsh and A. C. Howlett, *Pept. Sci.*, 2003, **71**, 169-189.
22. L. Padgett, A. Howlett and J.-Y. Shim, *J. Mol. Signal.*, 2008, **3**, 5.
23. O. M. H. Salo, M. Lahtela-Kakkonen, J. Gynther, T. Jarvinen and A. Poso, *J. Med. Chem.*, 2004, **47**, 3048-3057.
24. C. Montero, N. E. Campillo, P. Goya and J. A. Paez, *Eur. J. Med. Chem.*, 2005, **40**, 75-83.
25. T. Tuccinardi, P. L. Ferrarini, C. Manera, G. Ortore, G. Saccomanni and A. Martinelli, *J. Med. Chem.*, 2006, **49**, 984-994.
26. A. Gonzalez, L. S. Duran, R. Araya-Secchi, J. A. Garate, C. D. Pessoa-Mahana, C. F. Lagos and T. Perez-Acle, *Bioorg. Med. Chem.*, 2008, **16**, 4378-4389.
27. J.-Y. Shim, *Biophys. J.*, 2009, **96**, 3251-3262.
28. R. Ai and C.-E. A. Chang, *J. Mol. Graph. Model.*, 2012, **38**, 155-164.
29. G. N. Lee, K. R. Kim, S.-H. Ahn, M. A. Bae and N. S. Kang, *Bioorg. Med. Chem. Lett.*, 2010, **20**, 5130-5132.

30. H. Andersson, A. M. D'Antona, D. A. Kendall, G. Von Heijne and C.-N. Chin, *Mol. Pharmacol.*, 2003, **64**, 570-577.

31. J. F. Fay and D. L. Farrens, *Biochemistry*, 2013, **52**, 8286-8294.

32. R. Chenna, H. Sugawara, T. Koike, R. Lopez, T. J. Gibson, D. G. Higgins and J. D. Thompson, *Nucleic Acids Res.*, 2003, **31**, 3497-3500.

33. F. F. Davidson, P. C. Loewen and H. G. Khorana, *Proc. Natl. Acad. Sci. USA*, 1994, **91**, 4029-4033.

34. A. Šali, L. Potterton, F. Yuan, H. van Vlijmen and M. Karplus, *Proteins*, 1995, **23**, 318-326.

35. J. F. Fay, T. D. Dunham and D. L. Farrens, *Biochemistry*, 2005, **44**, 8757-8769.

36. K. H. Ahn, C. E. Scott, R. Abrol, W. A. Goddard and D. A. Kendall, *Proteins: Structure, Function and Bioinformatics*, 2013, **81**, 1304-1317.

37. R. A. Laskowski, M. W. MacArthur, D. S. Moss and J. M. Thornton, *J. Appl. Cryst.*, 1993, **26**, 283-291.

38. C.-H. Wu, M.-S. Hung, J.-S. Song, T.-K. Yeh, M.-C. Chou, C.-M. Chu, J.-J. Jan, M.-T. Hsieh, S.-L. Tseng, C.-P. Chang, W.-P. Hsieh, Y. Lin, Y.-N. Yeh, W.-L. Chung, C.-W. Kuo, C.-Y. Lin, H.-S. Shy, Y.-S. Chao and K.-S. Shia, *Journal of Medicinal Chemistry*, 2009, **52**, 4496-4510.

39. C.-M. Chu, M.-S. Hung, M.-T. Hsieh, C.-W. Kuo, S. T. D, J.-S. Song, H.-H. Chiu, Y.-S. Chao and K.-S. Shia, *Org. Biomol. Chem.*, 2008, **6**, 3399-3407.

40. J. Y. Kim, H. J. Seo, S.-H. Lee, M. E. Jung, K. Ahn, J. Kim and J. Lee, *Bioorg. Med. Chem. Lett.*, 2009, **19**, 142-145.

41. S. Y. Kang, S.-H. Lee, H. J. Seo, M. E. Jung, K. Ahn, J. Kim and J. Lee, *Bioorg. Med. Chem. Lett.*, 2008, **18**, 2385-2389.

42. R. L. Dow, P. A. Carpino, J. R. Hadcock, S. C. Black, P. A. Iredale, P. DaSilva-Jardine, S. R. Schneider, E. S. Paight, D. A. Griffith, D. O. Scott, R. E. O'Connor and C. I. Nduaka, *J. Med. Chem.*, 2009, **52**, 2652-2655.

43. H. Pettersson, A. Bülow, F. Ek, J. Jensen, L. K. Ottesen, A. Fejzic, J.-N. Ma, A. L. Del Tredici, E. A. Currier, L. R. Gardell, A. Tabatabaei, D. Craig, K. McFarland, T. R. Ott, F. Piu, E. S. Burstein and R. Olsson, *J. Med. Chem.*, 2009, **52**, 1975-1982.

44. P. A. Carpino, D. A. Griffith, S. Sakya, R. L. Dow, S. C. Black, J. R. Hadcock, P. A. Iredale, D. O. Scott, M. W. Fichtner, C. R. Rose, R. Day, J. Dibrino, M. Butler, D. B. DeBartolo, D. Dutcher, D. Gautreau, J. S. Lizano, R. E. O'Connor, M. A. Sands, D. Kelly-Sullivan and K. M. Ward, *Bioorg. Med. Chem. Lett.*, 2006, **16**, 731-736.

45. S. H. Lee, H. J. Seo, S.-H. Lee, M. E. Jung, J.-H. Park, H.-J. Park, J. Yoo, H. Yun, J. Na, S. Y. Kang, K.-S. Song, M.-A. Kim, C.-H. Chang, J. Kim and J. Lee, *J. Med. Chem.*, 2008, **51**, 7216-7233.

46. S. H. Lee, H. J. Seo, M. J. Kim, S. Y. Kang, K.-S. Song, S.-H. Lee, M. E. Jung, J. Kim and J. Lee, *Bioorg. Med. Chem. Lett.*, 2009, **19**, 1899-1902.

47. G. Murineddu, S. Ruiu, G. Loriga, I. Manca, P. Lazzari, R. Reali, L. Pani, L. Toma and G. A. Pinna, *J. Med. Chem.*, 2005, **48**, 7351-7362.

48. G. Murineddu, P. Lazzari, S. Ruiu, A. Sanna, G. Loriga, I. Manca, M. Falzoi, C. Dessì, M. M. Curzu, G. Chelucci, L. Pani and G. A. Pinna, *J. Med. Chem.*, 2006, **49**, 7502-7512.

49. Glide, Schrodinger, LLC, New York, NY, 2011.

50. Z. H. Song and T. I. Bonner, *Mol. Pharmacol.*, 1996, **49**, 891-896.

12

51. D. Hurst, U. Umejiego, D. Lynch, H. Seltzman, S. Hyatt, M. Roche, S. McAllister, D. Fleischer, A. Kapur, M. Abood, S. Shi, J. Jones, D. Lewis and P. Reggio, *J. Med. Chem.*, 2006, **49**, 5969-5987.

52. C.-N. Chin, J. Lucas-Lenard, V. Abadji and D. A. Kendall, *J. Neurochem.*, 1998, **70**, 366-373.

53. S. D. McAllister, G. Rizvi, S. Anavi-Goffer, D. P. Hurst, J. Barnett-Norris, D. L. Lynch, P. H. Reggio and M. E. Abood, *J. Med. Chem.*, 2003, **46**, 5139-5152.

54. MacroModel, Schrödinger, LLC, New York, NY, 2011.

13

Figure captions

Figure 1. The sequence alignment of CB1 with bovine rhodopsin used in our study. The transmembrane regions are colored in red and the identical residues in the transmembrane regions are marked in yellow. The identical residues in the regions outside the transmembrane regions are marked in cyan.

Figure 2. The superimposition of (a) 150 CB1 models and (b) TM1, (c) TM2, (d) TM3, (e) TM4, (f) TM5, (g) TM6 and (h) TM7 of all CB1 models.

Figure 3. A graphical illustration of the number of non-minimized (in green) and minimized (in orange) models that could dock a particular number of compounds from the small dataset of 72 CB1 antagonists. Only a few models could dock all (70-72) of the compounds.

Figure 4. The enrichment curves for the three best CB1 models. The two models that included minimization are shown in red and the model without minimization is shown in blue.

Figure 5. The obtained binding mode for rimonabant docked into the best CB1 model.

Figure 6. The obtained binding mode of a selected ligand that has a carboxamide functional group into the best CB1 model.

Figure 7. The obtained binding mode of a selected ligand that does not have a carboxamide functional group into the best CB1 model.
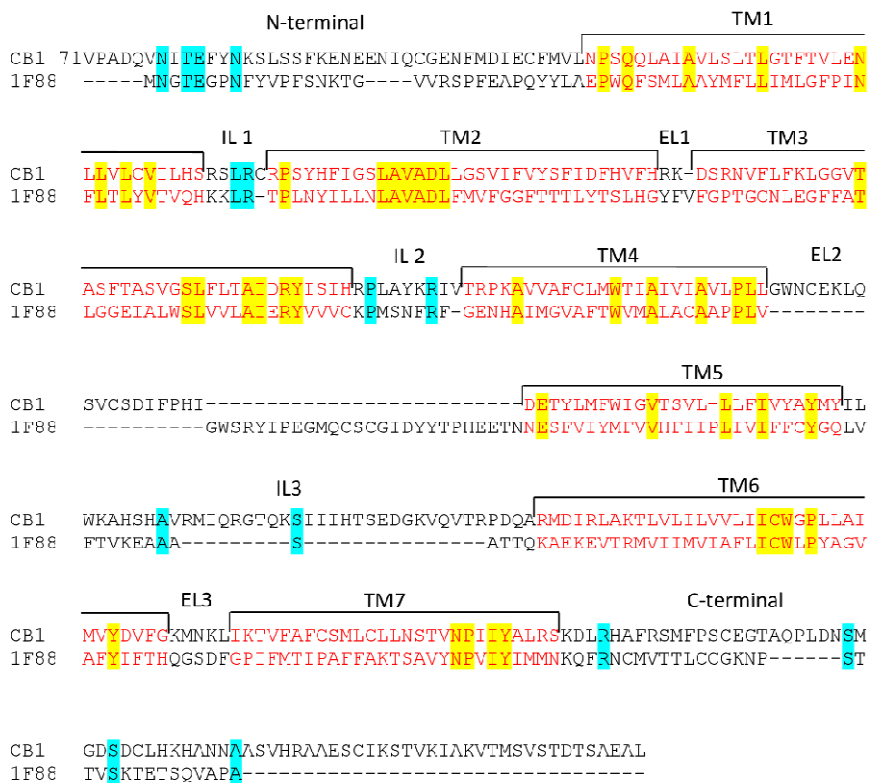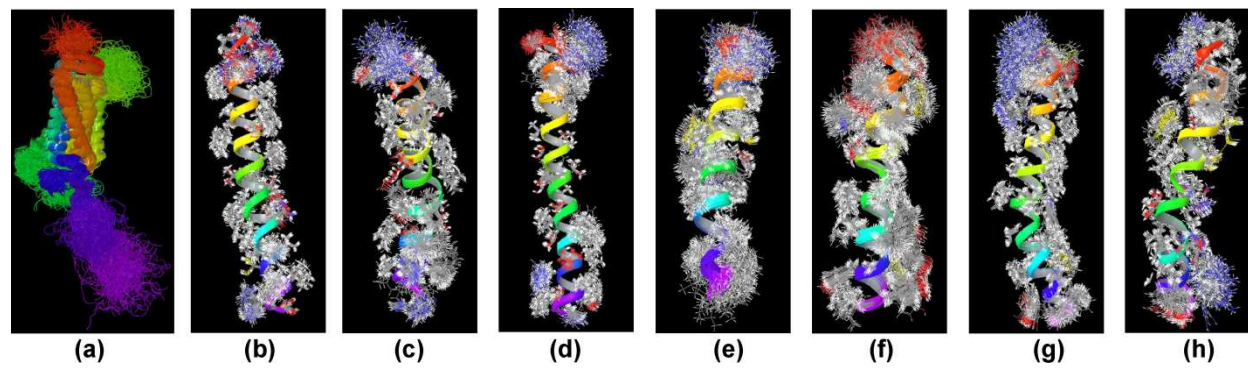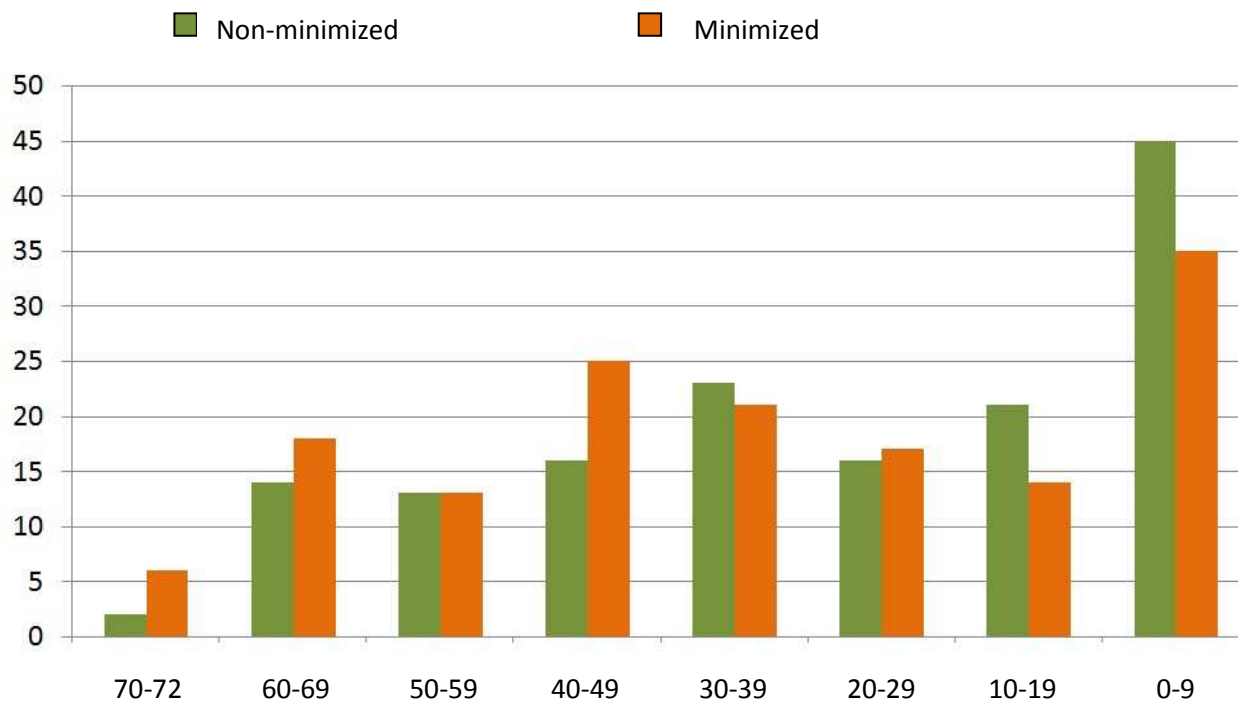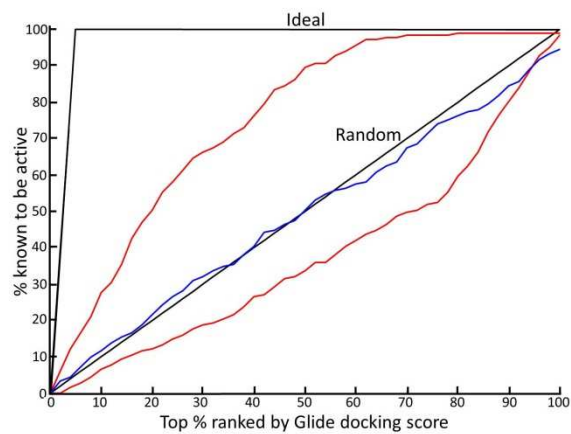
14

Figure 1.

15

(a)   (b)   (c)   (d)   (e)   (f)   (g)   (h)
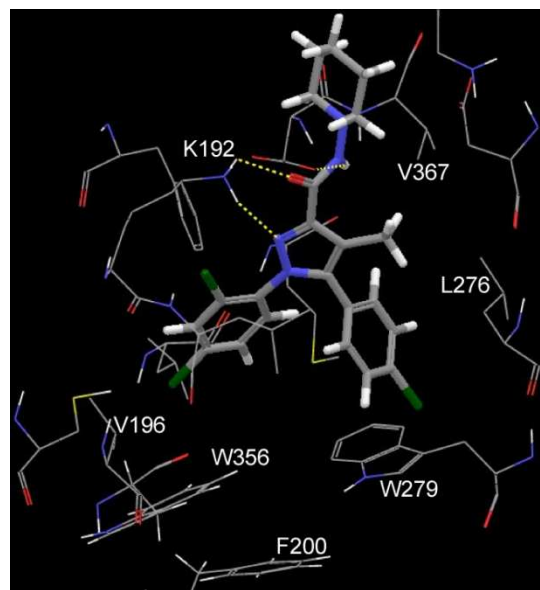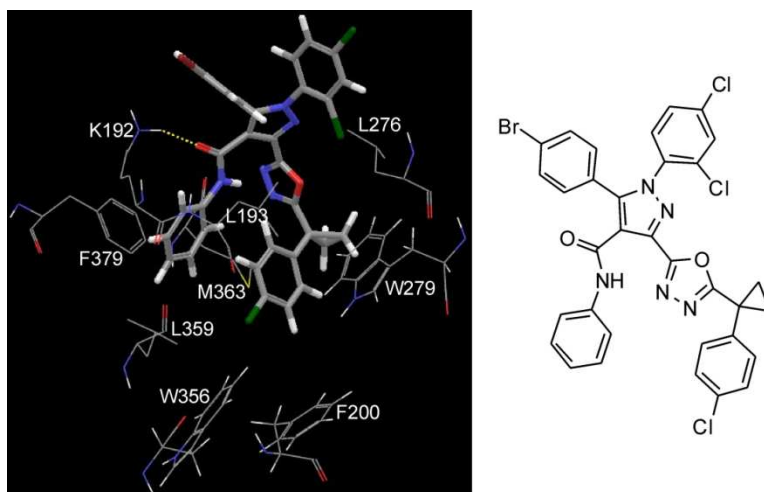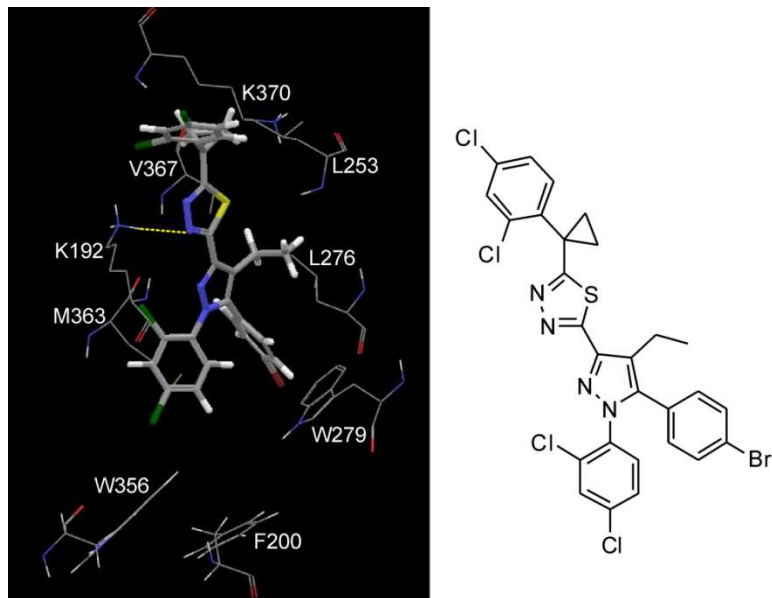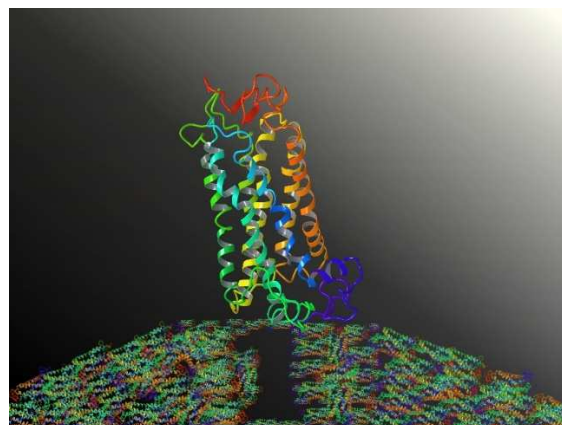
Figure 2.

16

Figure 3.

Figure 4.

18

Figure 5.

Figure 6.

Figure 7.

Table of Contents Graphic (could also be used as cover art)

Table of Contents Text:

Multiple cannabinoid 1 receptor models were prepared and the best one was selected based on the models' performance in selecting known ligands from a pool of competitors.